FEATURE-BASED MODULATION CLASSIFICATION USING CIRCULAR STATISTICS

Keith L. Davidson and
Jill R. Goldschneider
Insightful Corporation
1700 Westlake Avenue N., Suite 500
Seattle, Washington 98109

Luca Cazzanti and James W. Pitton
Applied Physics Laboratory
University of Washington
1013 NE 40th Street, Box 355640
Seattle, Washington 98105

ABSTRACT

In this paper we present a new set of signal features that can be used for modulation classification of digital communication signals in a blind environment. These new features are based on circular summary statistics taken from the instantaneous frequency of the sampled signal. The instantaneous frequency of a sampled baseband digital signal is expressed in radians. We consider the sampled instantaneous frequency as a set of realizations of a circular random variable and apply circular summary statistics to extract classification features. In particular, we use trigonometric moments of the instantaneous frequency to create feature vectors. We address the problem of distinguishing between FSK-type signals and QAM-type signals; and subsequently, the problem of discrimination between the FSK-type signals. We show that in both problems the signal classes are well separated in the circular statistics feature space and that automatic classifiers can be defined with simple thresholds.

I. INTRODUCTION

Blind demodulation systems for applications such as surveillance, threat identification, and electronic warfare are of great interest to the military. Accurate modulation classification of unidentified digital signals in a blind environment is a critical first step. Well known decision-theoretic based modulation classification techniques based on features extracted from the signal instantaneous amplitude, instantaneous phase, and/or instantaneous frequency have been proposed [1]–[3]. In this paper we present a simple decision-theoretic classification approach based on features extracted solely from the instantaneous frequency. This technique is unique in that we consider the instantaneous frequency of the sampled received baseband signal as realizations of a circulary-distributed random variable, and extract features using circular summary statistics. Unlike [1]–[3], our method can classify higher-order modulation and continuous phase signals by using features from the instantaneous frequency only.

We first address the problem of distinguishing between FSK-type signals and QAM-type signals. This coarse classification step is needed to choose the correct demodulation path in a blind demodulation system. The instantaneous frequency of FSK-type signals is, in general, a PAM signal which may or may not contain impulses depending on the continuity of the phase. The instantaneous frequency of QAM-type signals will always contain impulses at symbol transitions and is a function of the pulse shaping filter derivative within each symbol period. We will show that the features derived from circular summary statistics of the instantaneous frequency can be used to recognize this difference. We then address discrimination between the FSK-type signals. We will show that in both problems the signal classes are well separated in the circular statistics feature space and that automatic classifiers can be defined with simple thresholds.

The paper is organized as follows. In Section II we give a brief description of the circular summary statistics used for feature extraction. In Section III we show that the discrete instantaneous frequency of a complex baseband signal can be interpreted as a circular data set and give motivation for using it to classify FSK-type and QAM-type signals. In Section IV, we first present the new classification features, and then give synthetic and real-world examples of FSK-type and QAM-type classification and of classification among FSK-type modulations. Finally, concluding remarks are given in Section V.

II. CIRCULAR SUMMARY STATISTICS

Circular summary statistics are concerned with the statistical analysis of data samples that take angles as values. These data samples are realizations of a circularly-distributed random variable [4]. Analogous to linear statistics, moments of a circular random variable (trigonometric moments) are defined in terms of its probability density function. Measures of spread and symmetry, i.e., variance and skew, can be defined in terms of these moments. Circular kurtosis, a measure of peakedness in the circular density, can also be defined. As in the linear case, summary

statistics for circular data are used to compute estimates of theoretical values from samples of circular data. In this section we briefly describe the sample trigonometric moments and the corresponding variance, skew and kurtosis formulas. A more complete description of trigonometric moments and other statistical methods for circular data can be found in [4].
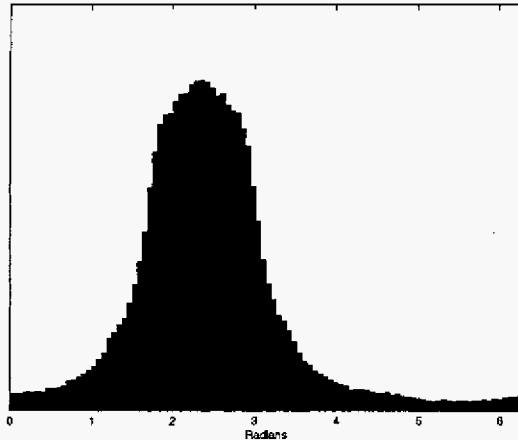
(a) Histogram of circular data.
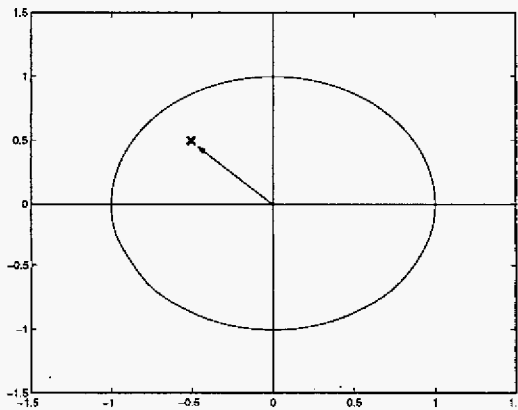
(b) First-order trigonometric moment, μ_1.

Fig. 1. (a) Histogram of circular data sample, Θ. The data is unimodal, and centered around 2.34 radians. (b) The complex first-order trigonometric moment, μ_1, of Θ. The mean direction, $\angle\mu_1$, gives the center of the unimodal data sample.

Sample Trigonometric Moments

Let $\Theta = \{\theta_k\}$ be a set of K data points in the range $[0, 2\pi)$. The first-order sample trigonometric moment of Θ is given by

$$\mu_1 = \frac{1}{K} \sum_{k=0}^{K-1} e^{j\theta_k}. \tag{1}$$

This complex number can be interpreted as the resultant vector sum of K unit vectors with angles given in Θ. This

resultant vector has length $|\mu_1|$ and lies at angle $\angle\mu_1$ in the complex plane. $\angle\mu_1$ is termed the *mean direction* of Θ. Figure 1(a) shows a histogram of an example data set Θ. Note that the abscissa is over the range $[0, 2\pi)$. It is constructive to picture the abscissa as *wrapped* around the unit circle. The data is unimodal, centered approximately at 2.4 radians. Figure 1(b) shows μ_1 (marked by ×) for this data in reference to the unit circle, where we see that μ_1 has an angle of approximately 135 degrees, or $\angle\mu_1 \approx 2.36$ radians.

In general, the pth-order sample trigonometric moment is given by

$$\mu_p = \frac{1}{K} \sum_{k=0}^{K-1} e^{jp\theta_k}, \tag{2}$$

and can be interpreted as the first-order moment of the data set Θ^p, defined by

$$\Theta^p \triangleq \{p \cdot \theta_k \mod 2\pi\}. \tag{3}$$

As in the case of linear statistics, measures of spread, symmetry, and peakedness in the underlying probability density can be defined in terms of these moments.

Circular Variance, Skew, and Kurtosis

Variance, skew, and kurtosis are descriptive statistics used for linear data that give, respectively, measures of the spread, symmetry, and peakedness of the underlying probability density of the data. These measures are also defined in the case of circular data. In terms of the sample trigonometric moments they are given by [4],

$$\text{(variance)} \quad \sigma^2 = 1 - |\mu_1| \tag{4}$$

$$\text{(skew)} \quad \gamma = |\mu_2| \sin\left(\angle\mu_2 - 2\angle\mu_1\right) / \left(\sigma^2\right)^{\frac{3}{2}} \tag{5}$$

$$\text{(kurtosis)} \quad \kappa = \left(|\mu_2| \cos\left(\angle\mu_2 - 2\angle\mu_1\right) - |\mu_1|^4\right) / \left(\sigma^2\right)^2. \tag{6}$$

The use of σ^2 to denote variance is strictly notational in this case. For circular data, the standard deviation is not the square root of σ^2, but is

$$\sigma = \sqrt{(-2\ln|\mu_1|)}. \tag{7}$$

III. INSTANTANEOUS FREQUENCY CLASSIFICATION FEATURES

To show how the trigonometric moments defined in the previous section can be applied to the instantaneous frequency of a signal, we start with a discrete-time model of the complex baseband signal,

$$s[n] = A(t)e^{j\varphi(t)}\Big|_{t=nT_s}, \tag{8}$$

where $A(t)$ and $\varphi(t)$ are, respectively, the instantaneous amplitude and instantaneous phase of the continuous-time

signal, and T_s is the sampling period. The instantaneous frequency of the signal is defined as the derivative of the instantaneous phase, $\varphi'(t)$. An approximation to the sampled instantaneous frequency, $\varphi'(nT_s)$, is given by

$$f[n] = \angle\, (s[n]s^*[n-1]) = \varphi\,[nT_s] - \varphi\,[(n-1)T_s]\,. \quad (9)$$

Note that $f[n]$ is in radians, with values in the interval $[0, 2\pi)$. Thus, $f[n]$ can be considered as circular data and the trigonometric moments defined in the previous section can be applied.

Figures 2 and 3 show the histograms of $f[n]$ for some of the digital signal types considered in this paper. Note the similarity of the QAM-type signals in Fig. 3. Qualitatively, these are distinctly different from the histograms for the FSK-type signals in Fig. 2. We next analyze $f[n]$ quantitatively, using trigonometric moments to distinguish signal classes.
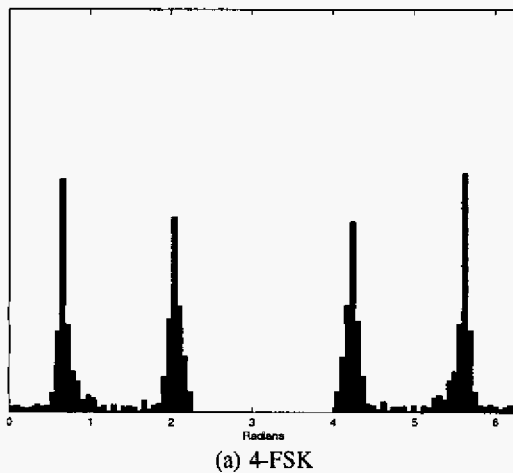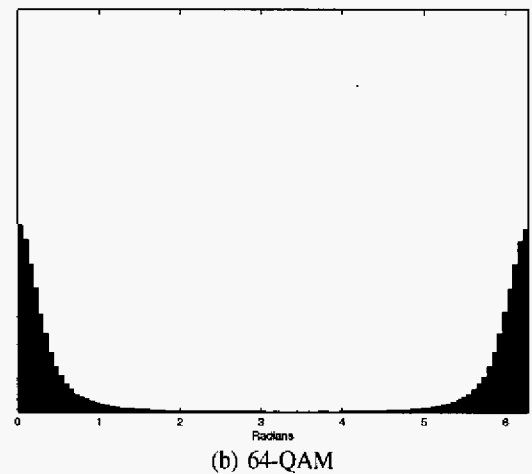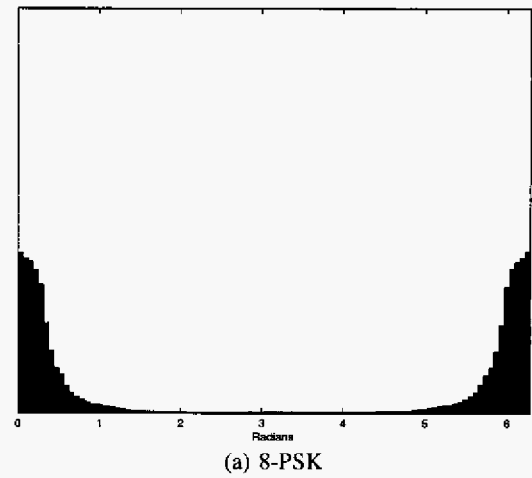

(a) 8-PSK

(b) 64-QAM

Fig. 3.   Instantaneous frequency histograms for 8-PSK and 64-QAM. These histograms are similar but distinctly different from the histograms of 4-FSK and GMSK shown in Fig. 2.

(a) 4-FSK

(b) GMSK

Fig. 2.   Instantaneous frequency histograms for 4-FSK and GMSK. As expected, "spikes" appear in the histograms due to the keying frequencies. This is in contrast to the "smooth" instantaneous frequency histograms of 8-PSK and 64-QAM shown in Fig. 3.

## IV. MODULATION CLASSIFICATION USING TRIGONOMETRIC MOMENTS

In this section we analyze the instantaneous frequency trigonometric moments of simulated and real-world FSK-type and QAM-type signals. We then show that features derived from these moments can be used for modulation classification. We first address coarse modulation classification, i.e., the problem of distinguishing FSK-type signals from QAM-type signals. The FSK-type signals we consider are (2,4)-FSK, (2,4)-CPM, MSK, and GMSK, and the QAM-type signals we consider are (2,4,8)-PSK and (16,32,64,256)-QAM. We then address *fine* modulation classification of the FSK-type signals, i.e., distinguishing among the FSK-types.
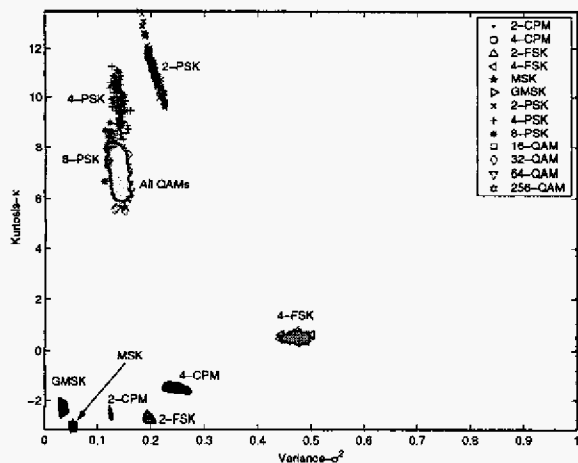
Classification of FSK-Type and QAM-Type Signals

We begin by simulating digital signals with:

1) Sampling frequency of 46387.33 Hz.
2) Symbol rate of 10 KHz, except for 2-CPM and 2-FSK, where the symbol rate is 5 KHz.
3) Root-raised cosine pulse shaping for all PSK, QAM and partial-response CPM signals (except GMSK), with rolloff of 0.35.

For each signal type, trigonometric moments are calculated for each of 113 data frames. The frame length is $K = 2048$ samples, approximately 440 symbols (220 symbols for 2-CPM and 2-FSK). Signals are generated at two SNR levels, 14 dB and 11 dB.
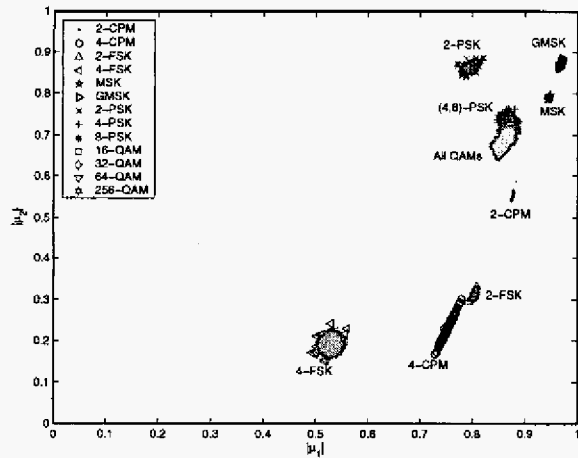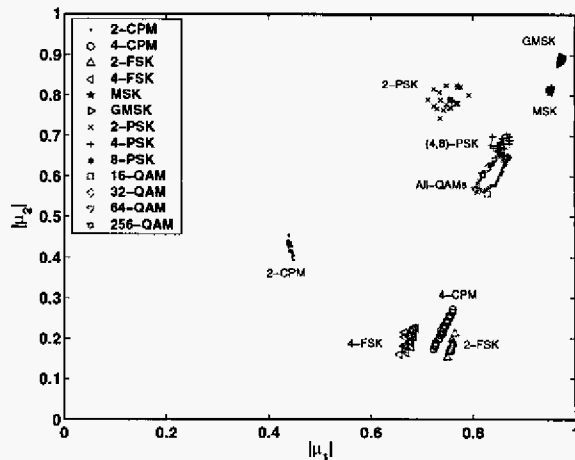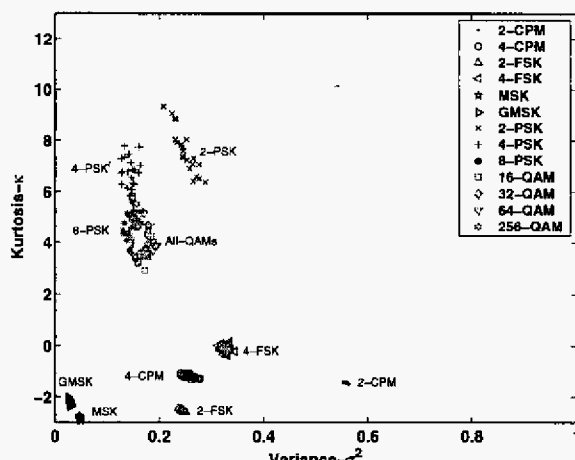

(a)

(b)

Fig. 4. (a) $|\mu_2|$ versus $|\mu_1|$ for simulated digital signals at 14 dB SNR. (b) Kurtosis versus variance. The FSK-type and QAM-type clusters are well separated in both planes. A simple 1-D classifier can be defined by thresholding the kurtosis at $\kappa = 3$.

In general, the directions of the trigonometric moments, $\angle\mu_p$, are clustered near zero or π for all signal types. This is due to circular symmetry in the instantaneous frequency of digital signals with respect to one of these
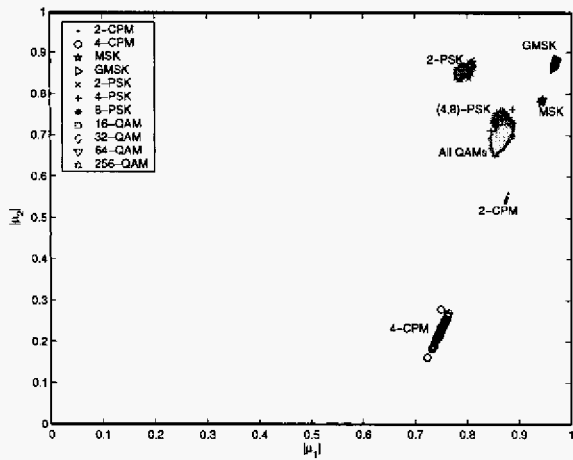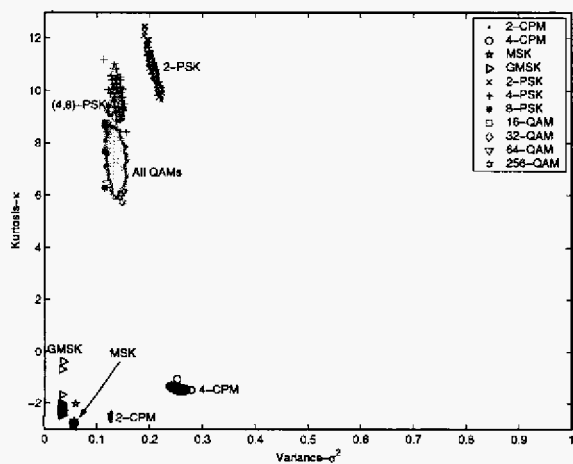

(a)

(b)

Fig. 5. (a) $|\mu_2|$ versus $|\mu_1|$ for simulated digital signals at 11 dB SNR. (b) Kurtosis versus variance. The FSK-type and QAM-type clusters are well separated in both planes. Even at this lower SNR a simple 1-D classifier can still be defined by thresholding the kurtosis at $\kappa = 3$.

points (see Figures 2 and 3). Thus we focus on the moment magnitudes, $|\mu_p|$. Figure 4(a) shows a plot of $|\mu_2|$ versus $|\mu_1|$ for all signals at SNR = 14 dB. Note the formation of distinct clusters for many signal types, e.g., 4-FSK, MSK, and 2-CPM. More importantly, for the purposes of coarse classification, there is no overlap of the FSK-type and QAM-type clusters. Figure 4(b) shows a plot of variance versus kurtosis, as computed using Eqs. (4) and (6), respectively. At this SNR we can define a simple 1-D coarse classifier to distinguish FSK-type from QAM-type signals by thresholding the kurtosis at $\kappa = 3$. Figure 5 shows the same results for signals at an SNR of 11 dB. At this lower SNR there is still no overlap between the FSK-type and QAM-type clusters, and the simple 1-D classifier defined by thresholding the kurtosis at $\kappa = 3$ remains valid.

(a)

(b)

Fig. 6. (a) $|\mu_2|$ versus $|\mu_1|$ for real-world digital signals at approximately 14 dB relative SNR. (b) Kurtosis versus variance. The results are nearly identical to those for simulated signals shown in Figure 4. The FSK-type and QAM-type clusters are well separated in both planes. A simple 1-D classifier can be defined by thresholding the kurtosis at $\kappa = 3$.

We now perform a similar analysis on real-world digital signals.[1] Figure 6 shows the trigonometric moment magnitudes for FSK-types (2,4)-CPM, MSK and GMSK, with QAM-types identical to that of the synthetic signals. The signal parameters of the real-world signals are identical to the synthetic signals, with approximate SNR of 11 dB. The results are comparable to the simulated results of Figure 4. Again, a 1-D classifier can be defined by thresholding the kurtosis at $\kappa = 3$.

It is important to note that in the above analysis of the real-world signals no attempt was made to remove any residual carrier. Indeed a coarse classifier defined in the

[1]All real-world signals used here were provided by Dr. Wei Su of U. S. Army RDECOM.

$|\mu_1|-|\mu_2|$ or $\sigma^2-\kappa$ planes would be invariant to the existence of constant residual carrier. To see this let $\tilde{s}(t)$ denote the baseband signal with residual carrier, i.e.,

$$\tilde{s}(t) = A(t)e^{j(\varphi(t)+\Omega_{rc}t)}, \qquad (10)$$

where Ω_{rc} is the residual carrier frequency in radians/sec. It follows from Eq. (9) that the approximate sampled instantaneous frequency of $\tilde{s}(n)$ is given by

$$\begin{aligned}
\tilde{f}[n] &= \angle\,(\tilde{s}[n]\tilde{s}^*[n-1]) \\
&= \varphi\,[nT_s] - \varphi\,[(n-1)T_s] + T_s\Omega_{rc} \\
&= f[n] + T_s\Omega_{rc}. \qquad (11)
\end{aligned}$$

Thus, the addition of residual carrier results in a *circular* shift of $f[n]$ by $T_s\Omega_{rc}$ radians. The histogram of $\tilde{f}[n]$ is a circularly shifted version of that for $f[n]$. The magnitudes of the trigonometric moments for $f[n]$ and $\tilde{f}[n]$ are thus identical. It follows from Eq. (4) that the variance is unaffected by circular shifts, and the same can be shown to be true for the kurtosis.

Effects of Pulse Shape Rolloff: The pulse-shaping filter for both the synthetic and real-world signals was a root-raised cosine with rolloff of 0.35. We now repeat the same analysis on synthetic signals generated with root-raised cosine filters of various rolloffs. Figure 7 shows the $\sigma^2 - \kappa$ feature space for rolloff values of 0.2, 0.5, and 0.9. We see that an increase in rolloff causes a decrease in kurtosis in the QAM-type signals. However, the FSK-type and QAM-type signals remain separated in the $\sigma^2 - \kappa$ plane. A threshold of $\kappa = 1$ can be used, at this SNR level, for all rolloff values if the median of the kurtosis over all signal frames is used as the classification feature.

Effects of Increased Noise Level: We now examine the effects of lower SNR on the trigonometric moment classification features. Figure 8 shows the results for real-world signals with approximate SNR of 5 dB. The increased noise level has, in general, increased the kurtosis of the FSK-type signals and decreased the kurtosis of the QAM-type signals. Although the FSK-type and QAM-type signals remain separated in the $\sigma^2 - \kappa$ plane, a simple 1-D classifier defined by thresholding the kurtosis is no longer possible. In this case a 2-D classifier must be employed.

Discrimination of FSK-Type Signals

After the received signal has been determined to be an FSK-type, a final classification decision must be made among the continuous-phase FSK-type signals. In this section, we show that the magnitudes of the first- and second-order trigonometric moments, $|\mu_1|$ and $|\mu_2|$, can be used for the classification of FSK-type signals.

Figure 9 shows a scatter plot of the first and second trigonometric moment magnitudes for real-world FSK-type

signals at approximately 14 dB and 11 dB. Four seconds of each signal type were segmented into frames of length 2048 (approximately 90 frames for each signal). The trigonometric moments were then computed for each frame. Four FSK signal types were tested: (2,4)-CPM, MSK, and GMSK. At these SNR levels the four signal types are clearly distinguishable in the $|\mu_1| - |\mu_2|$ feature space. Simple thresholds can be defined to distinguish the four signal types. MSK and GMSK can be distinguished from the CPM signals by thresholding $|\mu_2|$ at 0.62. Subsequently, MSK and GMSK can be distinguished by thresholding $|\mu_2|$ at 0.845. Finally, 2-CPM and 4-CPM are distinguished by thresholding $|\mu_1|$ at 0.57.

V. CONCLUSION

We have shown that trigonometric moments of the instantaneous frequency can be used to extract classification features from baseband digital signals. These features resulted in simple 1-D classifiers at moderate SNR levels. We used these features for coarse classification of FSK-type and QAM-type signals and for fine classification among the FSK-type signals. We found that these features were robust to higher-order modulations, e.g., 256-QAM, and constant carrier offset. We have also shown that the threshold in circular kurtosis for coarse classification is generally dependent on the pulse shape but that a single threshold can be used if the median circular kurtosis over a number of signal frames is taken as the classification feature. At low SNR, the signal classes remained separated in the feature space; however, non-linear classification techniques must be employed.

REFERENCES

[1] E. Azzouz and A. Nandi, "Automatic identification of digital modulations," *Signal Processing*, vol. 47, no. 1, pp. 55–69, 1995.

[2] ——, "Automatic modulation recognition—I," *Journal of the Franklin Institute*, vol. 334B, no. 2, pp. 241–273, 1997.

[3] A. A. Nandi and E. E. Azzouz, "Algorithms for automatic modulation recognition of communication signals," *IEEE Transactions on Communications*, vol. 46, no. 4, pp. 431–436, 1998.

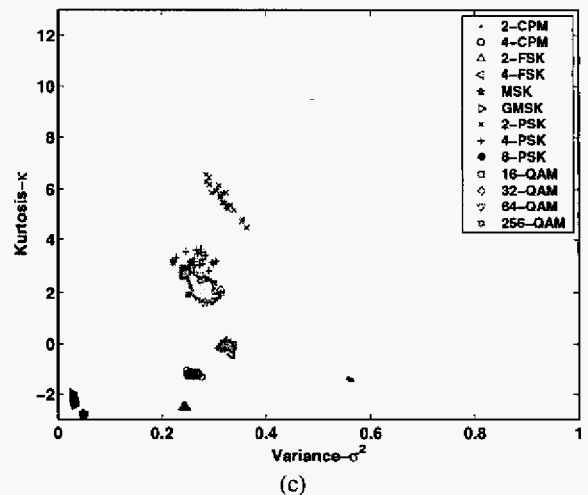[4] N. I. Fisher, *Statistical Analysis of Circular Data*. Cambridge University Press, 1995.
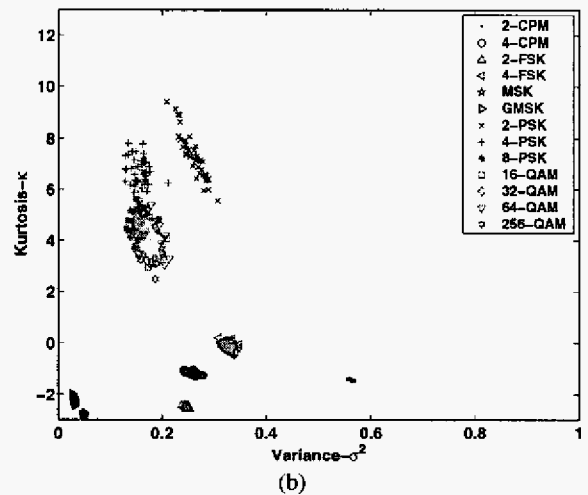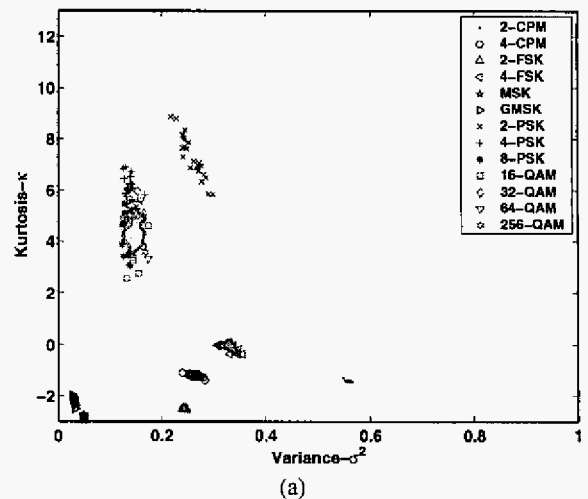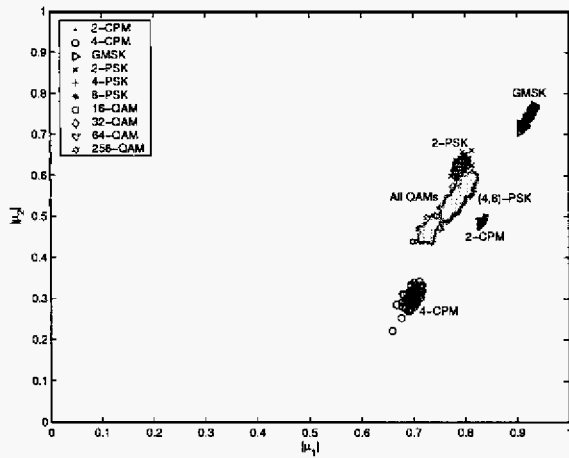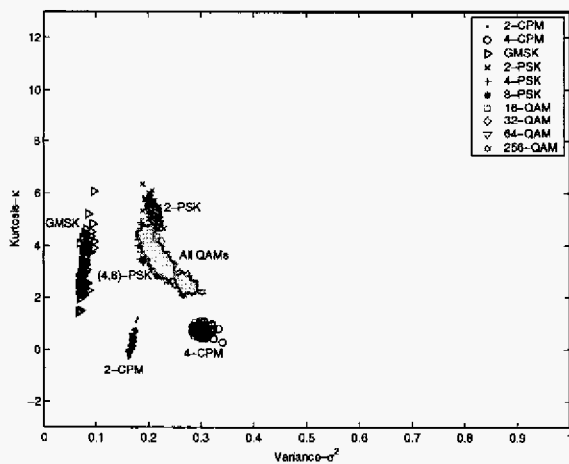
Fig. 7. The $\sigma^2 - \kappa$ feature space for synthetic signals generated with root-raised cosine filters with rolloff parameter values of (a) 0.2, (b) 0.5, and (c) 0.9.

(a)

(b)

Fig. 8. (a) $|\mu_1|$ versus $|\mu_1|$ for real-world digital signals at approximately 5 dB relative SNR. (b) Kurtosis versus variance. The FSK-type and QAM-type clusters remain well separated in both planes. A simple 1-D classifier defined by thresholding the kurtosis at $\kappa = 3$ is no longer possible. A robust 2-D classifier, however, can be defined.
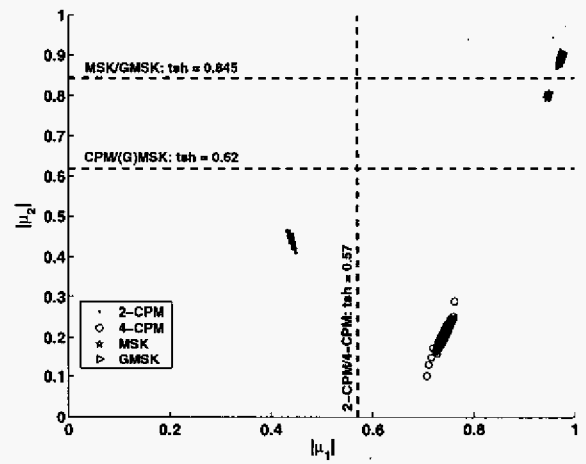

Fig. 9. The trigonometric moment feature space for classification of real-world FSK-type signals. Simple thresholds can be used for distinguishing: (G)MSK from CPM ($|\mu_2| = 0.62$); 2-CPM from 4-CPM ($|\mu_1| = 0.57$); and MSK from GMSK ($|\mu_2| = 0.845$).